VI. LABORATORY DISTRIBUTIONS

Laboratory distributions of the momenta and production angles of charged particles are shown in Figs. 12–17. All events except those including strange particles (2.1% of the total) and unassigned events (1.5% of the total) are included in these figures. The figures show the number of particles produced in a given interval of momentum or angle when a photon flux with the magnitude and energy distribution shown in Fig. 3 is passed through 1.04 g/cm^2 of hydrogen. This incident beam is nearly a bremsstrahlung distribution with a total energy of 2.04×10^8 BeV above 0.1 BeV, which is 3.71×10^7 equivalent quanta if a maximum energy of 5.5 BeV is chosen.

Single-prong events are included in Figs. 12–17 after scaling to the total flux for the rest of the sample.

Particles in the ambiguous events of the 0C multipion sample [reactions (4), (5), (7); and (8) of Table I] are also included; the ambiguous particle is placed in each possible mass category with a weight equal to the fraction predicted by a Monte Carlo calculation using phase-space distributions and applying the experimental criteria to the calculated sample.

The data of Figs. 12–17 are presented for their utility in estimating backgrounds or beam intensities available from photoproduction processes. The recent work done at DESY[15] is in agreement with these results.

ACKNOWLEDGMENTS

We wish to express our deep appreciation to the staff of the Cambridge Electron Accelerator for making the photon beam and the facilities of the CEA available. We wish also to thank our scanning groups for their efficient aid in the analysis of these data. We are indebted to our programming groups for the programming necessary for this experiment.

[15] Aachen-Berlin-Bonn-Hamburg-Heidelberg-München Bubble Chamber Collaboration, DESY 66/34, 1966 (unpublished).

PHYSICAL REVIEW VOLUME 155, NUMBER 5 25 MARCH 1967

π^+ Photoproduction from Hydrogen at Lab Angles from 34° to 155° and Lab Photon Energies from 500 to 1350 MeV*†

HENRY A. THIESSEN‡
California Institute of Technology, Pasadena, California
(Received 17 October 1966)

The differential cross section for the reaction $\gamma+p\rightarrow\pi^++n$ was measured using the Caltech 1.5-GeV electron synchrotron. The positive pions were detected and momentum analyzed in a multichannel magnetic spectrometer and the data were recorded in the memory of a pulse-height analyzer. The energy resolution was improved over previous experiments and an attempt was made to minimize systematic errors. The data are presented in the form of energy distributions at 12 lab angles from 34° to 155°, and the range of lab proton energies extended from 500 to 1350 MeV. Data were not taken at all energies for each angle, since the maximum useful momentum of the spectrometer, 600 MeV/c, restricted the maximum energy for lab angles less than or equal to 74°.

I. INTRODUCTION

THERE is presently considerable theoretical interest in photoproduction data, in part because of their importance in the evaluation of sum rules derived from the algebra of current components.[1–3] For these purposes, a detailed multipole and isotopic-spin decomposition of the photoproduction amplitudes is required. A phenomenological decomposition can be significant only if accurate and extensive data on differential cross sections are available, supplemented by data on recoil-nucleon polarization and polarized incident-photon asymmetries.

This paper reports the results of an experiment which was designed to measure the cross section for the reaction $\gamma+p\rightarrow\pi^++n$ at a large number of points with a minimum of systematic errors and good energy resolution. Measurements were made at pion lab angles from 34° to 155° and photon lab energies from 500 to 1350 MeV. The energy range was chosen to include the region in which the following resonant pion-nucleon states are important: $P_{11}(1400)$, $D_{13}(1518)$, $S_{11}(1550)$, $D_{15}(1688)$, and $F_{15}(1688)$.[4] Additional experiments and a phenomenological analysis of all existing data are in

* Work supported in part by the U. S. Atomic Energy Commission. Prepared under Contract No. AT(11-1)-68 for the San Francisco Operations Office, U. S. Atomic Energy Commission.

† This work is submitted in partial fulfillment of the requirements for the degree of Doctor of Philosophy at the California Institute of Technology.

‡ Present address: Los Alamos Scientific Laboratory, University of California, Los Alamos, New Mexico.

[1] A. Bietti, Phys. Rev. **142**, 1258 (1966).

[2] A. Bietti, Phys. Rev. **144**, 1289 (1966).

[3] F. Gilman and H. Schnitzer, Phys. Rev. **150**, 1362 (1966).

[4] P. Bareyere, C. Brickman, A. V. Stirling, and G. Villet, Phys. Letters **19**, 342 (1965).

progress at Caltech.[5] For this reason, no decomposition of the photoproduction amplitudes based on our data alone has been attempted.

This paper is divided into five parts. Section II is a summary of the experimental method. Section III is a description of the apparatus and the techniques used to calibrate it. Experimental checks on the operation of the apparatus are described in Sec. IV. Finally, the data and a comparison with previous results are presented in Sec. V.

II. EXPERIMENTAL METHOD

The reaction $\gamma+p\rightarrow\pi^++n$ was studied at the Caltech 1.5-GeV electron synchrotron. The bremsstrahlung beam illuminated a liquid-hydrogen target and the π^+ were detected and momentum analyzed in a magnetic spectrometer. The experimental method was similar to that used in several previous experiments.[6–11]

The kinematics of single-pion photoproduction relate the laboratory pion momentum p and angle θ to the laboratory photon energy k and c.m. pion angle $\theta_{\text{c.m.}}$. For two-pion production, as in the reactions

$$\begin{aligned}\gamma+p &\rightarrow \pi^++n+\pi^0\\ &\rightarrow \pi^++p+\pi^-,\end{aligned}$$

there is a minimum photon energy k_2 required to produce a π^+ with given laboratory angle and momentum, where $k_2>k$. In this experiment it was possible to choose E_0, the maximum energy of the photon spectrum, to lie between k and k_2 so that the multiple-pion reactions were not observed.

The background of particles incident on the spectrometer included protons, electrons, and muons. Protons were separated from pions in the counter system, while electrons and muons were indistinguishable from pions. Previous experiments showed that electron contamination at large angles from the photon beam was small, and several tests with the magnetic field reversed confirmed this result. The major source of muons was the decay of the pion $\pi^+\rightarrow\mu^++\nu$ and a correction for this process was made in computing the momentum resolution function (see Sec. III B). Muon pair production was assumed to be negligible.

Because k and $\theta_{\text{c.m.}}$ vary rapidly with p and θ, and because the spectrometer collected data in seven momentum channels simultaneously, it was not feasible to measure angular distributions at fixed values of k. Instead, the data were taken as energy scans at fixed laboratory angles. Several spectrometer central momentum settings were required for each scan, and an appropriate value of E_0 was chosen for each momentum setting.

The data were taken during two 4-month periods separated by 4 months. Each point was measured at least once during each period, and careful checks demonstrated that the two sets of data were consistent.

III. APPARATUS AND CALIBRATION

A. Photon Beam, Beam Monitors, and Hydrogen Target

The beam-area layout is shown schematically in Fig. 1. The electron beam of the Caltech synchrotron irradiated a 0.2 radiation length tantalum radiator and the resulting photon beam was collimated by a lead collimator to a rectangular cross section with half-angles of 1.8 and 2.2 mrad. The beam then passed through two lead scrapers (collimators with slightly larger apertures than the primary photon beam) and some sweeping magnets before striking the hydrogen target of another experiment. Two scrapers mounted in 6-in. lead walls served to eliminate particles produced in the upstream target before the beam reached our hydrogen target. The beam was stopped in a lead and concrete beam catcher 30 ft downstream from the liquid-hydrogen target.

The photon spectrum was computed from a thick-radiator bremsstrahlung theory developed by Wolverton at Caltech.[12] This theory combined the effects of showering and multiple scattering in the radiator to obtain the energy distribution as a function of angle. This distribution was integrated between limits defined by the primary collimator to obtain the bremsstrahlung spectrum. It is expected that the results of this calculation are accurate to 2%.

The primary standard for beam monitoring was a Wilson quantameter.[13] Because the beam spot was too large to put the quantameter downstream from the hydrogen target, we were unable to use the quantameter while taking pion data. Instead, the quantameter was located on a movable platform upstream of the hydrogen target. Before and after each data run, the quantameter was moved into the beam line and used to calibrate several secondary monitors consisting of two thin (0.005-in.-Al) ion chambers placed upstream from the quantameter and a monitor of the circulating beam of the synchrotron. By using this procedure, we believe that the average of the secondary monitors was calibrated with a precision of 0.5%, although the fluctua-

[5] S. D. Ecklund, C. R. Clinesmith, and R. L. Walker (private communications).
[6] F. P. Dixon and R. L. Walker, Phys. Rev. Letters 1, 142 (1958); 1, 458 (1958).
[7] J. R. Kilner, Ph.D. thesis, California Institute of Technology, 1963 (unpublished).
[8] L. Hand and C. Schaerf, Phys. Rev. Letters 6, 229 (1961).
[9] C. Schaerf, Nuovo Cimento 44, 504 (1966).
[10] H. Heinberg, W. M. McClelland, F. Turkot, W. M. Woodward, R. R. Wilson, and D. M. Zipoy, Phys. Rev. 110, 1211 (1958).
[11] S. D. Ecklund and R. L. Walter (private communication). An account of this experiment which measured the same reaction at forward angles is in preparation.
[12] An account of this work is in preparation. F. Wolverton kindly provided a computer program, BPAK I, which did the calculations.
[13] R. R. Wilson, Nucl. Instr. 1, 101 (1957).

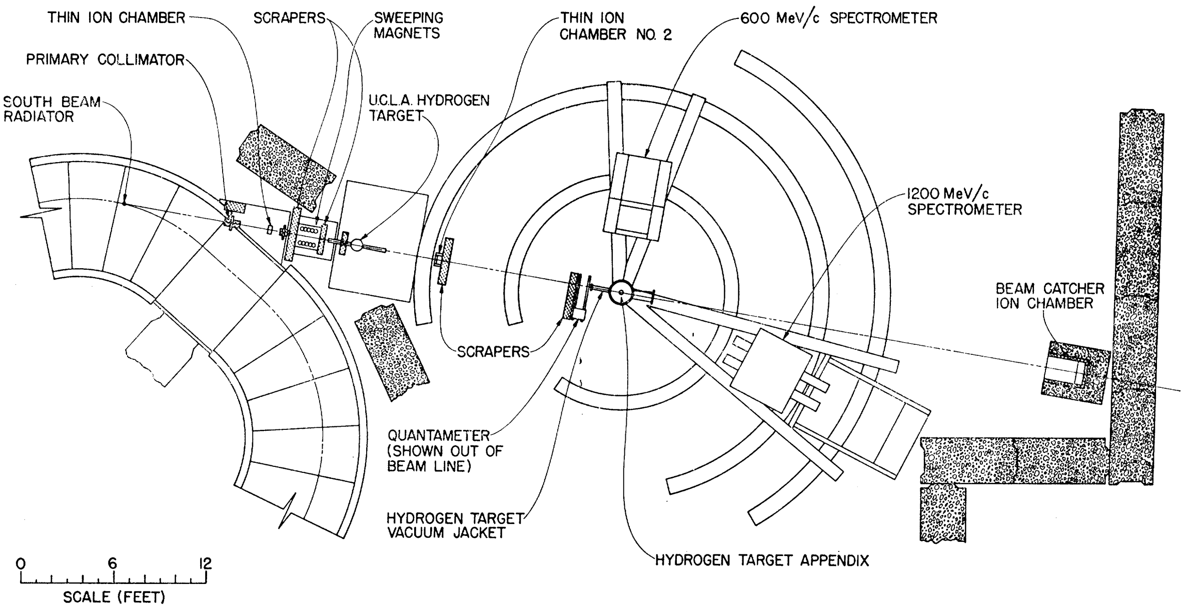

FIG. 1. Beam-area layout.

tions of a single secondary monitor were occasionally as large as 2%.

Shortly after all the data were obtained, the quantameter was taken to the Mark III linear accelerator at Stanford University and was calibrated with a Faraday cup. The result of this calibration was $U_Q = (4.78 \pm 0.15) \times 10^{18}$ MeV/C at the standard pressure and temperature of 800 mm Hg and 20°C. This number agrees very well with a previous experimental calibration[14] and with the theoretical value of 4.80×10^{18} MeV/C.[13] The theoretical constant has been used for normalizing the data presented here.

The liquid hydrogen was contained within a long, 3-in.-diam cylindrical cup of 0.005-in. Mylar with the axis of the cylinder perpendicular to the beam line. The beam spot size was 1.5×1.8 in. at the hydrogen target and was centered to within $\frac{1}{8}$ in. The location of the beam was verified frequently with Polaroid pictures. The spectrometer viewed the entire illuminated volume of the target at all laboratory angles.

B. The Magnetic Spectrometer

The spectrometer consisted of a wedge-shaped, uniform field magnet with a 4-in. gap (see Fig. 2). The radius of curvature was 47.25 in., the bending angle was 41.78°, and the maximum central momentum was 570 MeV/c. The magnetic field was continuously monitored with a nuclear-resonance magnetometer. The central momentum was measured as a function of the magnetometer frequency by floating-wire techniques with an absolute accuracy of better than 0.5%.

[14] R. Gomez, J. Pine, and A. Silverman, Nucl. Instr. Methods **24**, 429 (1963).

The solid angle accepted by the spectrometer was 3.27×10^{-3} sr and was defined by a thin scintillation counter placed near the rear edge of the magnetic field. The momentum acceptance was defined by a seven-channel hodoscope located at the focal plane. Each channel of this hodoscope accepted a 1.51% momentum interval. In order to measure the solid angle and momentum acceptance, a map of the magnetic field in the symmetry plane was made at values of the uniform field of 10 and 15 kG. The optical properties of the spectrometer were derived from the field-map data by numerical integration of the particle trajectories using a digital computer. The product of the solid angle and momentum acceptance obtained in this way was accurate to 1% after correcting for a 1.5% variation with the magnetic field near saturation. The central momentum calculated from the field maps agreed with the floating-wire measurements within 0.2%.

The calculation of the spectrometer acceptance was complicated by pion decay. Typically, 20% of the pions decayed in flight before reaching the last counter. Since pions and muons were indistinguishable in our counters, a Monte Carlo program was used to calculate the solid angle for accepting pions which decay. The results of this calculation also indicated that the decay process contributed long tails to the momentum resolution of the spectrometer.

Resolution functions for the seven momentum channels of the spectrometer at a typical setting are given in Fig. 3. The effects which have been included in the resolution calculation are beam size, nonlinear magnetic optics, pion decay, and multiple scattering. The resolution in lab photon energy calculated from these resolution functions varies from 15 MeV at the

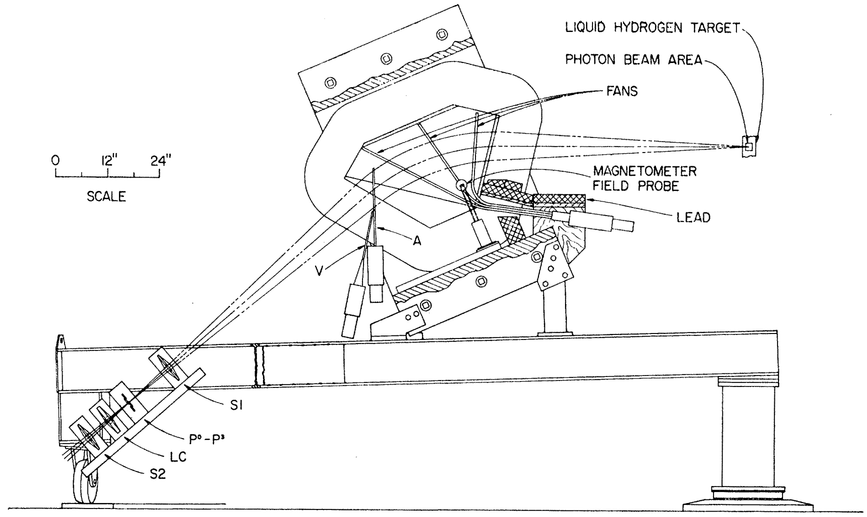

FIG. 2. 600-MeV/c spectrometer and counters.

smallest angle and lowest energy to 110 MeV at the largest angle and highest energy. More detailed information about the energy resolution of this experiment is presented in Fig. 4.

C. Counters

Ten scintillation counters and one Čerenkov counter were mounted on the spectrometer as shown in Fig. 2. The aperture counter (A) was made from $\frac{1}{8}$-in. NE-102 plastic and was mounted on a long, thin Plexiglas light pipe. To eliminate events which result from particles passing through the light pipe or the phototube, a large scintillation counter (V) shielded the light pipe and phototube and was put into anticoincidence with A. Similarly, a counter ("fan") was mounted on each pole face to guard against charged particles scattered by the iron.

The remaining seven counters, placed near the momentum focus at the rear of the spectrometer, consisted of two scintillation counters S1 and S2, a Plexiglas threshold Čerenkov counter LC, and a four-counter, seven-channel hodoscope P^i. Because of the defocusing effect of the magnet fringing fields, the rear counters were long (15 in.) in the direction parallel to the uniform magnetic field. Counters LC, S1, and S2 had a phototube mounted at each end to improve the uniformity of pulse height and timing response.

D. Electronics

The electronics were divided into three independent subsystems: a fast logic system containing conventional coincidence modules; a pulse-height analysis system consisting of linear gates and discriminators; and a data-storage system which made use of a Nuclear Data 1024-channel pulse-height analyzer and a special integrated-circuit control system. For each event, nine digital signals from the fast-logic and pulse-height-analysis systems defined a nine-bit binary number which completely specified the event. Events of each logic type were accumulated in the cell of the pulse-height-analyzer memory addressed by their binary number. The remaining half of the memory was used to collect a pulse-height distribution from any one of the counters for diagnostic purposes. After each run, the

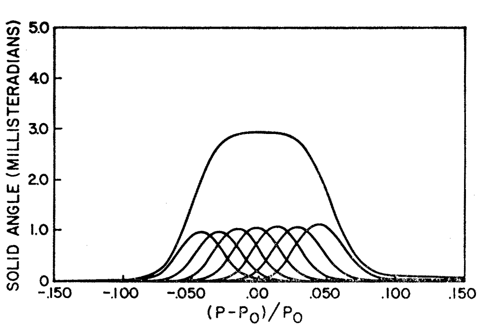

FIG. 3. Momentum-resolution functions for the seven channels of the spectrometer. The upper curve is the sum of the other curves. These functions vary slowly with the central momentum P_0, and these curves were calculated for $P_0=400$ MeV/c.

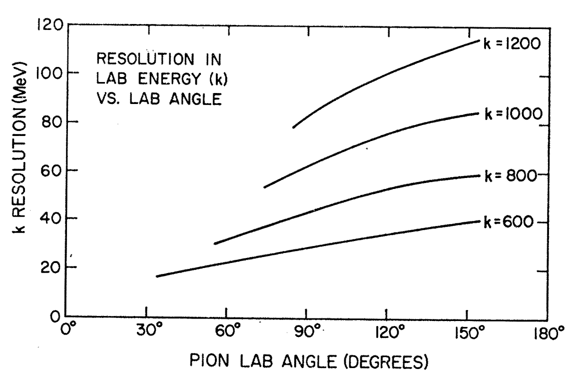

FIG. 4. Resolution in lab photon energy (full width at half-maximum) versus pion lab angle.

contents of the memory were punched on paper tape and processed by an IBM 7094 computer.

Pions were separated from protons by crude time-of-flight requirements, by dE/dx selection in counters S1 and S2, and by velocity selection in counter LC. There was enough redundancy in the system to permit monitoring the pion and proton efficiencies for each run. In addition, accidentals in counter A and in the momentum hodoscope P^i were monitored during each run.

IV. EXPERIMENTAL TESTS

A. Backgrounds

The empty-target background was measured at each point. In each case, an empty-target run was made within a few days of the full-target run to correct for a possible buildup of solid substances on the Mylar cup of the target. The empty-target yield was typically 4% of the full-target yield, and in no case was it greater than 11%.

Several tests were made with the magnetic field reversed to look for electron contamination. Under these conditions, the only single-pion-photoproduction reaction which can contribute is

$$\gamma+n\rightarrow\pi^-+p\,,$$

and these events can be produced only in the target walls. Experimentally, it was found that about half of the reversed field events resulted from the empty target. The remaining events typically amounted to 1–3% of the full-target π^+ rates, but for the highest energies this rate increased to as much as 10%. No satisfactory explanation for these events was found. It was demonstrated that only a small fraction of these events could be due to any one of the following sources: wide-angle pair production, conversion of high-energy photons from π^0 decay in the target structure, high-energy electrons from the Dalitz decay of π^0's, conversion of low-energy photons in the aperture counter, or pions from multiple-pion photoproduction which were counted because of the long tails of the momentum-resolution function. It was possible that a small contribution from each of these factors could have explained these events. The difference between the full-target and empty-target reversed-field counting rates was assumed to be a smooth function of lab angle and was subtracted from the π^+ rate. This assumption was consistent with all the data taken with magnet field reversed. In order to indicate the possible errors of this procedure, an error of half of this correction was added in quadrature with the statistical error when the error flags of all cross sections were computed.

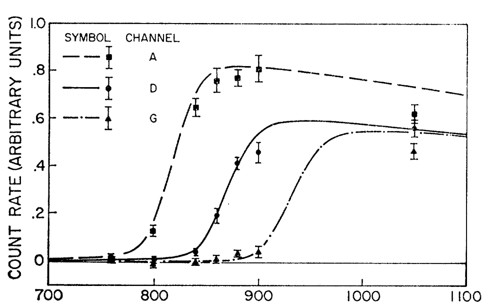

FIG. 5. Photon excitation functions measured at 64.0° lab. The results for three of the seven momentum channels are shown. The smooth curves are calculated from the cross sections reported in Table I, the momentum-resolution functions of the spectrometer, and the bremsstrahlung spectrum computed by the program BPAK I (Ref. 11).

B. Photon Excitation Functions

Two photon excitation functions were measured during the course of the experiment. For these tests, the spectrometer momentum and angle were held constant and the counting rate in each of the seven channels was measured as a function of the synchrotron energy E_0. The results for a typical case, shown in Fig. 5, indicate that the reaction has been properly identified, that a small (1±1%) background exists below threshold, and that the experimental resolution has been accurately calculated.

C. Nuclear Interactions

The inefficiency caused by nuclear interaction of pions was measured by inserting additional matter at various positions in the system. These measurements were made at 300 and 500 MeV/c. For matter between the hydrogen target and counter S1, the loss of events was consistent with known total cross sections.[15–19] The loss due to matter in the region near the momentum focus decreased approximately linearly with the distance to the last counter; the loss near counter S2 was approximately 0.4 of the loss at counter S1. The loss of events was approximately a factor of 2 greater at 300 MeV/c than at 500 MeV/c. The inefficiency was assumed to have the momentum dependence of the total cross section of pions scattered from an appropriate mixture of hydrogen and light nuclei, and was normalized to give the best fit to the 300- and 500-MeV/c measurements. The result of this calculation is shown in Fig. 6. The accuracy of this procedure was 25%, which leads to a maximum error of 3% in the cross section.

[15] N. I. Petrov, V. G. Ivanov, and V. A. Rusakov, Zh. Eksperim. i Teor. Fiz. **37**, 957 (1959) [English transl.: Soviet Phys.—JETP **10**, 682 (1960)].
[16] A. G. Meshkovskii and Ya. Ya. Shalamov, Zh. Eksperim. i Teor. Fiz. **37**, 978 (1959) [English transl.: Soviet Phys.—JETP **10**, 697 (1960)].
[17] M. P. Balandin, O. I. Ivanov, V. A. Moiseenko, and G. L. Sokolov, Zh. Eksperim. i Teor. Fiz. **46**, 415 (1964) [English transl.: Soviet Phys.—JETP **19**, 279 (1964)].
[18] J. W. Cronin, R. Cool, and A. Abashin, Phys. Rev. **107**, 1121 (1957).
[19] F. Jacob and G. Chew, *Strong Interaction Physics* (W. A. Benjamin, Inc., New York, 1964).

D. Reproducibility

In order to test the reproducibility of cross-section measurements in this experiment, a standard point was measured every few days during the second data-taking period. A Plexiglas target with the same geometry as the liquid-hydrogen target was used to increase the counting rate. A total of 18 such runs were taken. The standard deviation of the results was 2.06% when 1.23% was expected from the counting statistics alone. No satisfactory explanation of this discrepancy was found. A random error of 1.65% was added in quadrature with the statistical error of each run to correct for this effect.

V. RESULTS AND CONCLUSIONS

The data are tabulated in Table I and are plotted in Fig. 7. These data are plotted in the form of energy

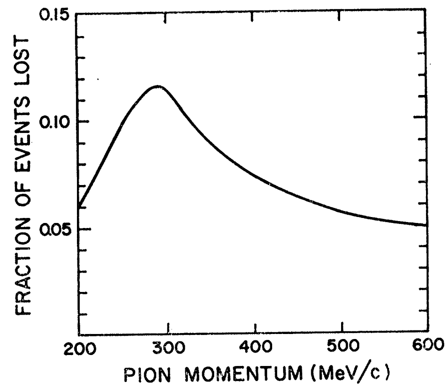

FIG. 6. Loss of events due to nuclear interactions with the matter through which the detected pions passed.

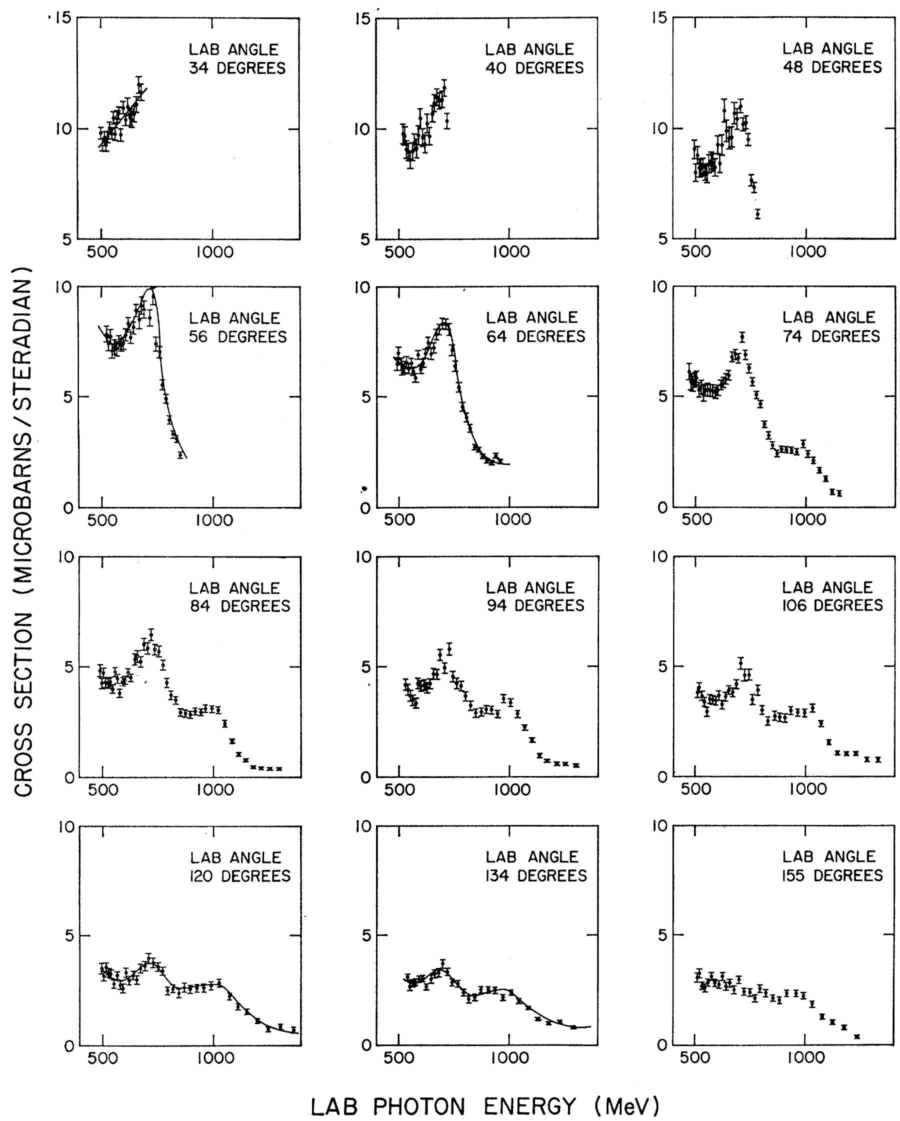

FIG. 7. The differential cross section in the c.m. system for the reaction $\gamma+p\rightarrow\pi^++n$. Smooth curves have been drawn through some of the data for purposes of comparison with other experiments in Fig. 8. See Table II for a discussion of experimental errors.

TABLE I. The differential cross section in the c.m. system for the reaction $\gamma+p\rightarrow\pi^{+}+n$. W is the invariant mass, k is the lab photon energy, and $\theta_{c.m.}$ is the pion c.m. angle relative to the photon. See Table II for a list of experimental errors.

θ_{lab} (deg)	W (MeV)	k (MeV)	$\theta_{c.m.}$ (deg)	$d\sigma/d\Omega$ (μb/sr)	θ_{lab} (deg)	W (MeV)	k (MeV)	$\theta_{c.m.}$ (deg)	$d\sigma/d\Omega$ (μb/sr)	θ_{lab} (deg)	W (MeV)	k (MeV)	$\theta_{c.m.}$ (deg)	$d\sigma/d\Omega$ (μb/sr)
34.0	1354	508	48.6	9.79±0.29		1462	670	80.5	8.48±0.38		1655	991	107.1	2.88±0.17
	1359	515	48.8	9.29±0.28		1469	682	80.8	9.15±0.39		1668	1014	107.6	2.40±0.16
	1364	522	48.9	9.58±0.28		1477	694	81.0	8.96±0.39		1682	1039	108.0	2.13±0.14
	1369	530	49.1	9.25±0.27		1485	706	81.3	10.03±0.40		1697	1065	108.5	1.69±0.13
	1374	538	49.2	9.63±0.27		1494	720	81.6	8.59±0.37		1712	1093	108.9	1.31±0.12
	1380	546	49.4	10.03±0.27		1502	734	81.9	9.58±0.38		1728	1123	109.4	0.72±0.11
	1386	555	49.6	9.77±0.26		1511	748	82.3	7.40±0.32		1746	1155	109.9	0.66±0.12
	1392	564	49.7	10.50±0.29		1522	765	82.6	7.04±0.26	84.0	1339	487	106.2	4.79±0.26
	1397	572	49.9	9.76±0.29		1530	779	82.9	5.56±0.23		1345	496	106.4	4.24±0.23
	1403	580	50.1	10.54±0.29		1539	793	83.3	4.89±0.21		1352	505	106.6	4.69±0.24
	1409	589	50.2	10.71±0.29		1548	808	83.6	3.95±0.18		1358	514	106.8	4.24±0.22
	1415	598	50.4	9.71±0.27		1558	825	83.9	3.29±0.17		1365	524	107.1	4.23±0.21
	1421	608	50.6	10.95±0.29		1568	841	84.3	3.06±0.16		1372	535	107.3	4.31±0.21
	1428	617	50.8	10.41±0.27		1578	859	84.6	2.37±0.14		1380	545	107.6	3.98±0.20
	1435	629	51.0	11.02±0.38	64.0	1346	496	85.4	6.51±0.29		1387	556	107.9	4.74±0.20
	1441	638	51.2	10.51±0.38		1351	504	85.7	7.00±0.28		1394	567	108.1	4.44±0.20
	1447	648	51.3	10.43±0.37		1357	513	85.9	6.53±0.27		1402	578	108.4	3.79±0.18
	1454	658	51.5	10.66±0.36		1363	521	86.1	6.26±0.26		1409	589	108.7	4.31±0.18
	1461	668	51.7	11.09±0.36		1370	531	86.3	6.37±0.26		1418	602	109.0	4.39±0.18
	1468	679	51.9	11.98±0.37		1376	540	86.6	6.59±0.26		1426	615	109.3	4.72±0.19
	1475	690	52.1	11.65±0.36		1383	550	86.8	6.32±0.25		1435	628	109.6	4.48±0.18
40.0	1366	525	57.0	9.76±0.44		1391	562	87.1	6.56±0.20		1446	645	109.9	5.32±0.25
	1371	533	57.1	9.67±0.43		1397	571	87.4	6.18±0.20		1454	658	110.2	5.47±0.26
	1376	540	57.3	9.05±0.40		1404	581	87.6	5.86±0.19		1463	672	110.5	5.22±0.25
	1382	549	57.5	8.94±0.41		1411	591	87.9	6.93±0.20		1473	687	110.9	6.02±0.26
	1388	557	57.7	8.58±0.38		1418	602	88.2	6.26±0.19		1483	702	111.2	5.84±0.25
	1394	566	57.9	8.95±0.39		1425	614	88.4	6.55±0.19		1493	719	111.6	6.46±0.26
	1400	576	58.1	9.38±0.37		1433	626	88.7	6.99±0.19		1504	736	111.9	5.78±0.24
	1407	585	58.3	9.11±0.44		1442	639	89.0	7.50±0.24		1516	756	112.3	5.70±0.24
	1412	594	58.5	9.71±0.44		1449	650	89.3	6.97±0.24		1526	773	112.7	5.08±0.23
	1418	603	58.7	10.48±0.44		1457	662	89.6	7.24±0.24		1537	791	113.0	4.26±0.20
	1425	613	58.9	9.60±0.41		1465	675	89.9	7.86±0.24		1549	810	113.4	3.70±0.19
	1431	623	59.1	9.30±0.41		1474	688	90.2	8.07±0.24		1561	830	113.8	3.46±0.17
	1438	633	59.3	10.24±0.43		1482	702	90.5	8.34±0.25		1574	851	114.2	2.92±0.17
	1445	644	59.5	9.66±0.41		1491	716	90.9	8.31±0.24		1587	874	114.6	2.87±0.15
	1453	656	59.8	10.68±0.37		1501	732	91.2	8.08±0.27		1601	896	115.0	2.80±0.17
	1459	666	60.0	11.16±0.39		1510	746	91.5	7.13±0.25		1613	918	115.4	2.95±0.17
	1466	677	60.2	11.43±0.38		1519	760	91.8	6.40±0.24		1627	941	115.8	2.91±0.16
	1473	688	60.4	11.29±0.37		1528	776	92.2	5.44±0.21		1641	966	116.3	3.08±0.16
	1480	699	60.6	11.34±0.37		1538	792	92.5	4.55±0.19		1656	993	116.7	3.07±0.16
	1488	711	60.9	11.85±0.38		1548	809	92.9	4.08±0.18		1672	1021	117.2	3.02±0.16
	1496	723	61.1	10.34±0.35		1559	826	93.3	3.58±0.17		1689	1051	117.7	2.42±0.14
48.0	1345	496	66.5	9.00±0.42		1572	847	93.7	2.72±0.12		1707	1085	118.2	1.62±0.09
	1350	503	66.7	7.97±0.39		1582	864	94.1	2.61±0.11		1724	1114	118.7	1.02±0.08
	1356	510	66.9	8.75±0.39		1592	882	94.4	2.30±0.11		1741	1146	119.2	0.76±0.07
	1361	518	67.1	8.17±0.38		1603	901	94.8	2.11±0.10		1759	1180	119.7	0.44±0.06
	1367	527	67.3	8.21±0.39		1615	921	95.2	2.01±0.10		1778	1216	120.2	0.41±0.06
	1373	535	67.5	8.21±0.38		1627	942	95.6	2.33±0.10		1799	1255	120.8	0.38±0.06
	1379	544	67.7	7.98±0.36		1640	964	96.0	2.06±0.09		1820	1297	121.3	0.37±0.06
	1386	554	67.9	7.90±0.41	74.0	1333	477	95.8	6.14±0.37	94.0	1371	532	116.7	4.16±0.25
	1391	563	68.1	8.35±0.41		1338	485	96.0	5.67±0.36		1378	542	116.9	3.93±0.25
	1397	571	68.3	8.49±0.40		1344	493	96.2	5.59±0.34		1385	553	117.2	3.67±0.23
	1404	581	68.6	8.40±0.40		1350	502	96.4	5.78±0.35		1393	565	117.4	3.45±0.23
	1410	591	68.8	8.20±0.39		1356	511	96.7	5.85±0.33		1401	577	117.7	3.33±0.22
	1417	601	69.0	9.23±0.41		1363	521	96.9	5.32±0.34		1410	590	118.0	4.21±0.24
	1424	611	69.3	8.37±0.38		1370	531	97.2	5.44±0.31		1419	603	118.3	4.09±0.22
	1431	622	69.5	9.21±0.48		1377	541	97.4	5.10±0.27		1427	617	118.6	4.16±0.23
	1437	632	69.7	10.77±0.52		1383	550	97.7	5.29±0.26		1436	630	118.8	4.02±0.23
	1444	642	70.0	9.85±0.50		1390	560	97.9	5.36±0.26		1445	643	119.1	4.21±0.23
	1451	653	70.2	9.53±0.48		1397	571	98.2	5.31±0.25		1454	658	119.4	4.66±0.23
	1459	665	70.5	9.57±0.46		1404	582	98.5	5.28±0.25		1464	674	119.7	4.64±0.23
	1466	676	70.7	10.65±0.49		1412	594	98.7	5.19±0.25		1475	690	120.1	5.54±0.24
	1474	689	71.0	10.39±0.47		1420	606	99.0	5.30±0.24		1486	708	120.4	4.93±0.23
	1483	703	71.3	10.97±0.31		1429	620	99.4	5.56±0.22		1499	729	120.8	5.79±0.26
	1490	715	71.6	10.15±0.30		1437	631	99.7	5.66±0.23		1510	746	121.2	4.53±0.24
	1498	727	71.8	10.24±0.29		1445	644	100.0	5.83±0.23		1521	764	121.5	4.24±0.23
	1506	739	72.1	9.46±0.27		1453	657	100.3	5.98±0.22		1533	783	121.9	4.10±0.22
	1514	753	72.4	7.63±0.24		1462	670	100.6	6.81±0.23		1545	804	122.2	3.63±0.20
	1523	767	72.7	7.29±0.23		1471	685	100.9	6.93±0.23		1558	825	122.6	3.20±0.19
	1532	781	73.0	6.10±0.21		1481	700	101.2	6.76±0.22		1572	848	123.0	2.87±0.18
56.0	1366	525	77.0	7.84±0.36		1491	716	101.6	7.71±0.22		1588	875	123.5	2.91±0.17
	1371	533	77.2	7.43±0.34		1500	730	101.9	6.91±0.21		1601	898	123.9	3.02±0.18
	1377	542	77.4	7.71±0.34		1510	746	102.3	6.30±0.20		1616	922	124.3	3.01±0.17
	1383	551	77.6	7.09±0.33		1520	762	102.6	5.69±0.19		1631	948	124.7	2.84±0.17
	1390	560	77.9	7.26±0.32		1530	779	103.0	5.08±0.17		1647	976	125.1	3.52±0.17
	1396	570	78.1	7.20±0.32		1541	797	103.4	4.67±0.16		1664	1006	125.6	3.33±0.17
	1403	580	78.4	7.47±0.32		1553	816	103.8	3.76±0.15		1682	1038	126.1	2.83±0.15
	1411	592	78.6	7.34±0.27		1565	836	104.2	3.26±0.17		1699	1070	126.6	2.22±0.12
	1417	601	78.9	7.47±0.28		1576	854	104.5	2.80±0.16		1717	1102	127.0	1.66±0.11
	1424	611	79.1	7.83±0.27		1587	873	104.9	2.43±0.14		1735	1135	127.5	0.95±0.09
	1431	622	79.4	8.33±0.28		1599	894	105.3	2.62±0.15		1755	1172	128.0	0.71±0.08
	1438	633	79.6	7.69±0.26		1612	915	105.7	2.61±0.14		1776	1212	128.5	0.59±0.07
	1446	645	79.9	8.14±0.27		1625	938	106.2	2.58±0.14		1798	1254	129.0	0.57±0.07
	1454	657	80.2	8.90±0.27		1639	962	106.6	2.51±0.14		1822	1300	129.6	0.51±0.08

TABLE I. (*continued*).

θ_{lab} (deg)	W (MeV)	k (MeV)	$\theta_{c.m.}$ (deg)	$d\sigma/d\Omega$ (μb/sr)	θ_{lab} (deg)	W (MeV)	k (MeV)	$\theta_{c.m.}$ (deg)	$d\sigma/d\Omega$ (μb/sr)	θ_{lab} (deg)	W (MeV)	k (MeV)	$\theta_{c.m.}$ (deg)	$d\sigma/d\Omega$ (μb/sr)
106.0	1357	512	126.7	3.79±0.23		1401	577	139.1	2.74±0.19		1541	796	151.9	2.38±0.16
	1364	522	126.9	4.00±0.22		1410	590	139.4	2.60±0.19		1555	820	152.2	2.06±0.14
	1371	533	127.1	3.64±0.21		1419	604	139.6	3.33±0.20		1571	846	152.4	2.16±0.15
	1379	544	127.4	3.36±0.21		1429	619	139.8	2.95±0.19		1588	874	152.7	2.51±0.15
	1387	556	127.6	2.90±0.19		1439	635	140.1	3.19±0.19		1606	905	153.0	2.51±0.14
	1396	569	127.9	3.48±0.19		1450	651	140.3	2.97±0.19		1625	938	153.3	2.50±0.41
	1405	582	128.1	3.43±0.19		1462	669	140.6	3.50±0.19		1646	974	153.6	2.17±0.14
	1415	597	128.4	3.41±0.21		1475	690	140.9	3.62±0.21		1666	1010	153.9	2.41±0.10
	1423	611	128.7	3.63±0.22		1486	707	141.2	3.97±0.22		1687	1047	154.2	2.00±0.10
	1432	624	129.0	3.22±0.20		1498	726	141.4	3.77±0.20		1709	1087	154.5	1.69±0.09
	1442	639	129.2	3.59±0.20		1511	747	141.7	3.57±0.19		1733	1131	154.8	1.21±0.08
	1453	655	129.5	3.89±0.20		1524	769	142.0	3.40±0.18		1759	1179	155.2	1.01±0.07
	1463	672	129.8	3.79±0.20		1539	792	142.3	2.48±0.17		1787	1232	155.5	1.09±0.07
	1475	690	130.1	4.16±0.21		1554	818	142.6	2.58±0.16		1817	1290	155.9	0.83±0.07
	1486	708	130.5	5.11±0.27		1569	843	143.0	2.38±0.20	155.4	1355	510	163.6	3.09±0.20
	1497	725	130.8	4.58±0.26		1584	868	143.3	2.65±0.20		1363	522	163.7	3.29±0.19
	1508	743	131.1	4.60±0.25		1600	895	143.6	2.54±0.19		1372	534	163.8	2.71±0.18
	1521	763	131.4	3.46±0.22		1617	924	143.9	2.57±0.18		1381	547	163.9	2.62±0.17
	1534	785	131.7	3.88±0.22		1635	956	144.3	2.60±0.19		1390	561	164.0	2.85±0.17
	1547	807	132.1	2.99±0.21		1655	990	144.7	2.71±0.19		1400	576	164.1	3.15±0.17
	1562	831	132.5	2.49±0.18		1675	1027	145.1	2.83±0.18		1411	592	164.2	2.83±0.16
	1580	861	132.9	2.74±0.19		1701	1073	145.6	2.23±0.15		1422	609	164.3	2.78±0.18
	1594	885	133.3	2.66±0.19		1722	1111	145.9	1.75±0.15		1433	625	164.4	3.14±0.18
	1609	910	133.7	2.63±0.18		1744	1152	146.3	1.52±0.13		1444	642	164.5	2.69±0.17
	1625	938	134.1	2.96±0.18		1768	1197	146.8	1.12±0.11		1456	660	164.6	2.83±0.18
	1642	968	134.5	2.86±0.17		1795	1247	147.2	0.73±0.10		1468	680	164.7	2.52±0.16
	1661	1000	134.9	2.85±0.18		1823	1301	147.7	0.84±0.12		1482	701	164.9	2.98±0.18
	1680	1035	135.4	3.08±0.18		1853	1361	148.2	0.70±0.14		1496	724	165.0	2.43±0.16
	1702	1075	135.9	2.37±0.13	134.0	1377	541	149.0	3.06±0.17		1513	750	165.1	2.40±0.17
	1721	1110	136.3	1.52±0.11		1385	554	149.1	2.65±0.16		1527	773	165.3	2.13±0.16
	1742	1147	136.8	1.04±0.10		1394	567	149.3	2.81±0.16		1542	798	165.4	2.57±0.17
	1764	1189	137.2	1.00±0.09		1403	581	149.5	2.86±0.16		1558	825	165.6	2.37±0.16
	1787	1234	137.7	1.03±0.09		1413	596	149.7	3.00±0.15		1576	854	165.7	2.14±0.15
	1813	1282	138.3	0.76±0.09		1424	611	149.9	3.02±0.15		1594	886	165.9	2.04±0.15
	1840	1334	138.8	0.73±0.11		1435	628	150.1	2.64±0.14		1615	920	166.0	2.36±0.15
120.0	1343	492	137.7	3.51±0.22		1448	648	150.3	3.00±0.17		1637	960	166.2	2.35±0.15
	1349	501	137.9	3.15±0.19		1459	665	150.5	3.25±0.18		1658	995	166.4	2.23±0.15
	1357	512	138.1	3.55±0.20		1470	683	150.7	3.28±0.18		1679	1034	166.5	1.84±0.13
	1365	523	138.3	3.31±0.19		1482	702	150.9	3.67±0.18		1703	1077	166.7	1.29±0.11
	1373	535	138.5	3.27±0.18		1496	723	151.2	3.33±0.17		1729	1125	166.9	1.03±0.10
	1381	548	138.7	2.79±0.18		1509	745	151.4	2.83±0.16		1757	1177	167.1	0.80±0.09
	1390	561	138.9	3.18±0.17		1524	769	151.7	2.78±0.15		1788	1234	167.3	0.36±0.08

distributions at fixed angles. The angular distributions are in good agreement with previous data[20] and are not presented here.

In calculating these cross sections, the effects of the long tails of the momentum-resolution function were unfolded. This correction was based on the observed energy dependence of the cross section and the tails of the resolution function computed by the Monte Carlo method. The magnitude of this correction was less than 3% in the worst case.

The systematic error not included in the error bars is estimated to be 5%, and this error is to be interpreted in the sense of a standard deviation. The three largest contributors to this error are the quantameter calibration (3%), the correction for nuclear interactions (3%), and the bremsstrahlung spectrum (2%). A complete list of the experimental errors is presented in Table II.

A comparison with other data[6–8,10,11,21–23] is presented in Fig. 8. In general, our data agree satisfactorily with the previous results. There are, however, two serious

TABLE II. Summary of experimental errors (standard deviations).

Random errors included in error flags	
Counting statistics	3–5%
Field-reversed background	0–5%
Reproducibility	1.65%
Unfolding	1%
Systematic errors in addition to error flags	
Nuclear interactions	3%
Quantameter calibration	3%
Bremsstrahlung spectrum	2%
Magnet calibration	1%
Decay correction	1%
Hydrogen-target parameters	1%
Electronic efficiency	1%
Total (assuming Gaussian statistics)	5%

[20] S. D. Ecklund and R. L. Walker, in *Proceedings of the International Symposium on Electron and Photon Interactions at High Energies*, edited by G. Hohler (Deutsche Physikalische Gesellschaft, Hamburg, 1966), Vol. II. A compilation of all available data including the results of the present experiment appears in J. T. Beale, S. D. Ecklund, and R. L. Walker, Report No. CTSL-42, California Institute of Technology, Pasadena, California, 1966 unpublished).

[21] R. L. Walker, J. G. Teasdale, V. Z. Peterson, and J. I. Vette, Phys. Rev. **99**, 210 (1955).

[22] A. V. Tollestrup, J. E. Keck, and R. M. Worlock, Phys. Rev. **99**, 220 (1955).

[23] J. Bizot, J. Perez y Jorba, and D. Trielle, in *Proceedings of the International Symposium on Electron and Photon Interactions at High Energies*, edited by G. Hohler (Deutsche Physikalische Gesellschaft, Hamburg, 1966), Vol. II.

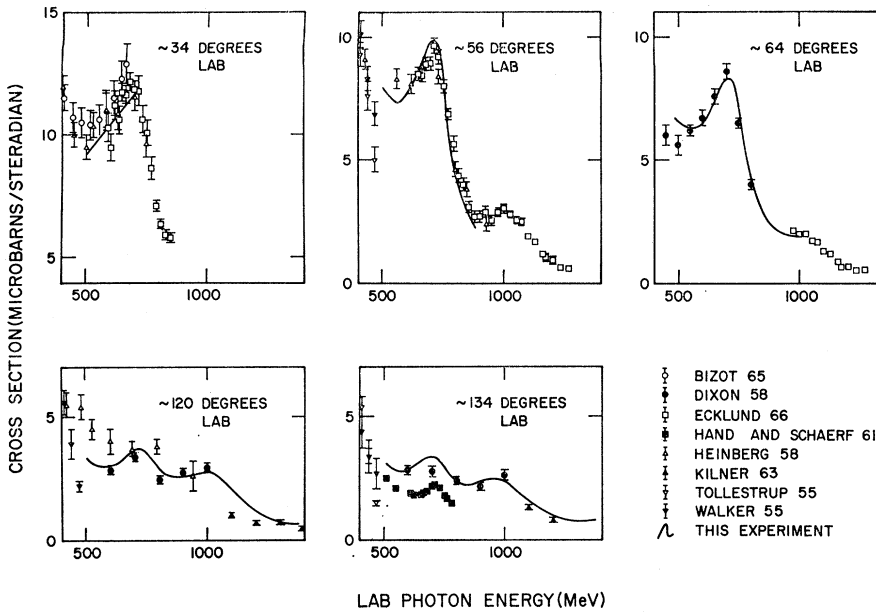

FIG. 8. A comparison of the data of this experiment with those of other experiments. The data are taken from Refs. 6, 7, 8, 10, 11, 21, 22, and 23. The smooth curves are also shown in Fig. 7.

discrepancies. The first occurs in the region between 400 and 600 MeV, where there is only a limited amount of data. The two early experiments at Caltech done by Walker *et al.*[21] and Tollestrup *et al.*[22] give systematically 20–50% smaller results than our data. We believe that in the early experiments the synchrotron energy was too close to k, and that their results are in error at 440 and 470 MeV. An experiment covering the energy region of 400 to 600 MeV and a wide angular range should be done to check this discrepancy and to fill a gap in the data. This experiment cannot be performed at Caltech at the present time because of difficulties with operating the synchrotron at low energies.

Our data at a lab angle of 134° are in serious disagreement with the data of Hand and Schaerf at 135°.[8] The two experiments agree on the energy dependence of the cross section, but the data of Hand and Schaerf must be multiplied by a scale factor of 1.5 ± 0.1 to be brought into agreement with our data. A photon excitation curve was measured at 134° lab near a k of 700 MeV (see Sec. IV B). The below-threshold background at this point was $1\pm1\%$, which demonstrates that no serious background is included in our data. Thus, we believe that their data are incorrectly normalized. The same scale factor of 1.5 should be used for their 180° data and the later data of Schaerf.[9]

ACKNOWLEDGMENTS

I am very grateful to my supervisor, Professor R. L. Walker, for his support and helpful criticism. I wish to thank M. G. Hauser, who contributed many useful discussions and spent many hours taking data. I would like to acknowledge several enlightening conversations with S. D. Ecklund, Dr. J. O. Maloy, Dr. J. H. Mullins, and Dr. C. Peck. The assistance of the synchrotron technical staff was greatly appreciated.

Professor J. Pine helped with the quantameter calibration. I would also like to thank D. Quinn and the staff of the Mark III linear accelerator at Stanford University for their cooperation during this calibration.

Finally, I gratefully acknowledge the financial support of the National Science Foundation and the U. S. Atomic Energy Commission.